Dalton Transactions

Accepted Manuscript

ROYAL SOCIETY OF CHEMISTRY

www.rsc.org/dalton

Graphic Abstract

Six copper(II) complexes containing tridentate polypyridyl ligand showed significant DNA binding/cleavage activity and remarkable anticancer potency with low IC_{50} values.

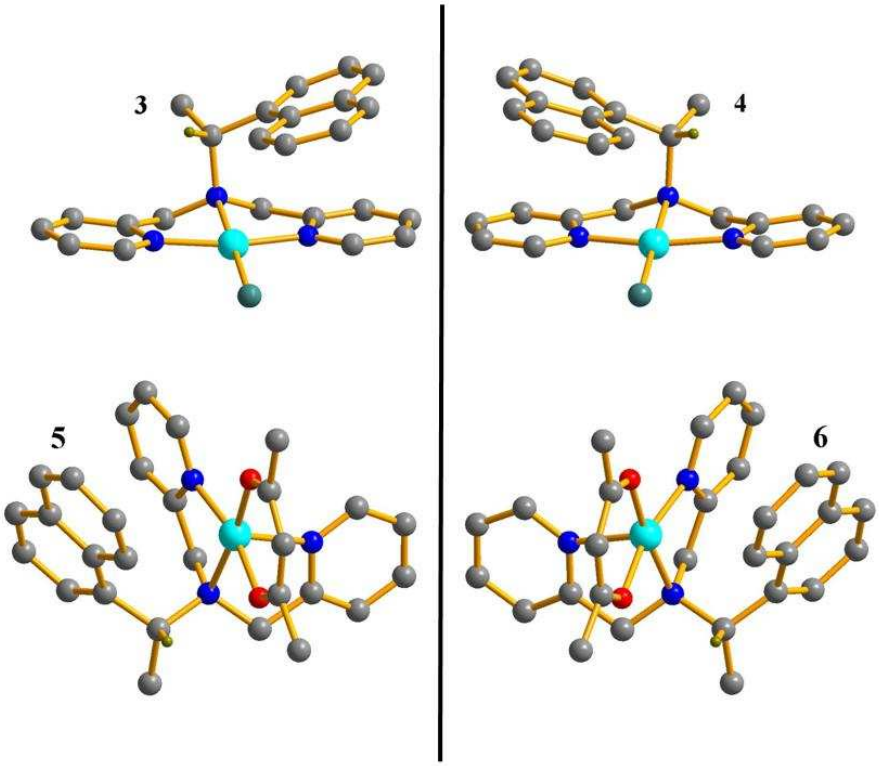

Cite this: DOI: 10.1039/c0xx00000x

www.rsc.org/xxxxxx

ARTICLE TYPE

Synthesis, Characterization, DNA/BSA interactions and Anticancer Activity of achiral and chiral copper complexes

Xue-Quan Zhou,[a,b,c] Qian Sun,[a,b] Lin Jiang,[a,b] Si-Tong Li,[a] Wen Gu,[a,b] Jin-Lei Tian,*[a,b,c] Xin Liu,[a,b] and Shi-Ping Yan[a,b]

Received (in XXX, XXX) Xth XXXXXXXXX 20XX, Accepted Xth XXXXXXXXX 20XX
DOI: 10.1039/b000000x

Six novel copper(II) complexes of $[CuL^1Cl]ClO_4$ (**1**), $[CuL^1(acac)]PF_6$ (**2**), $[CuL^{2(R)}Cl]_2(PF_6)_2$ (**3**), $[CuL^{2(S)}Cl]_2(PF_6)_2$ (**4**), $[CuL^{2(R)}(acac)]PF_6$ (**5**) and $[CuL^{2(S)}(acac)]PF_6$ (**6**), (L^1 = 1-naphthyl-N,N- [bis(2-pyridyl)methyl]amine, L^2 = R/S-1-naphthyl-N,N-[bis(2-pyridyl)methyl]ethanamine, acac = diacetone) were synthesized to serve as artificial nucleases. All complexes were structurally characterized by X-ray crystallography. The crystal structures showed the presence of distorted square-planar CuLCl (**1**, **3** and **4**) and distorted tetragonal-pyramidal CuL(acac) (**2**, **5** and **6**) geometry. The interaction of these complexes with CT-DNA was researched by means of several spectroscopy methods, which indicated that complexes bound to CT-DNA by intercalation binding mode. DNA cleavage experiments revealed that the complexes exhibited remarkable DNA cleavage activities in the presence of H_2O_2, and single oxygen ($^1O_2$) or hydroxyl radical may serve as the major cleavage active species. Especially, the *in vitro* cytotoxicity of the complexes on four human cancer cells lines (HeLa, MCF-7, Bel-7404 and HepG-2) demonstrated that the six compounds had broad-spectrum anti-cancer activity with low IC_{50} values. The stronger cytotoxicity and DNA cleavage activity of chiral enantiomers compared with achiral analogues verified the influence of chirality in antitumor activity of complexes. Meanwhile, the protein binding ability was revealed by quenching of tryptophan emission with the addition of complexes using BSA as a model protein. The results indicated that quenching mechanisms of BSA by the complexes were static process.

Introduction

DNA contains the main genetic materials controlling the protein synthesis, cell proliferation and the growth of organisms.[1-5] DNA can work naturally in healthy cells, but several cancer cells have the ability to suppress and invade the normal cells by such characteristics as unlimited reproduction, transform, and metastasis due to the mutation of DNA.[6-11] Thus numerous scientists have transferred their research direction into the mechanism of cancer, the precaution and therapy of tumor.[12-18]

Metal complex acting as anticarcinogen attracted much sight since the invention of cisplatin, a DNA targeting drug which could destroy the regeneration of cancers' DNA.[19-22] In the meantime, cisplatin showed a powerful defence against sarcoma, lymphoma and germinoma, etc.[19,23-26] While much side-effects such as emesis, nephrotoxicity, and neurotoxicity restricted its comprehensive application in the therapy of cancers.[21,26] Considering the imperfection of platinum-based drugs, transition metal complexes were synthesized and tested for their potential anticancer activities and low toxicities. Notably, copper complexes were regarded as better candidates of anticarcinogen because copper(II) ion played crucial role in many biomolecules such as ceruloplasmin and tyrosinase.[27-31]

In the field of copper complexes acting as DNA targeting drugs and anticarcinogen, a kind of copper complexes derived from polypyridine ligands played increasingly important roles because of the aromaticity and strong coordination ability with copper(II), resulting in favorable interaction with DNA, mainly including intercalation and groove binding.[31-35] A series of copper(II) complexes $[CuL^a(X)][ClO_4]$ (L^a = 2-((2-phenyl-2-(pyridin-2-l)hydrazono)-methyl)pyridine, X = N_3, SCN, OAc, OBz, CN, H_2O, ClO_4) showed different DNA binding ability and antiproliferative effects which were consistent with those similar copper complexes already published, and all complexes exhibited enhanced cytotoxicity in MCF-7, PC-3, and HEK 293 cells

[a] *College of Chemistry, Collaborative Innovation Center of Chemical Science and Engineering (Tianjin), Nankai University, Tianjin 300071, China, E-mail: tiant@nankai.edu.cn*
[b] *Tianjin Key Laboratory of Metal and Molecule Based Material Chemistry, Tianjin 300071, China*
[c] *Key Laboratory of Advanced Energy Materials Chemistry (MOE), Tianjin 300071, China*

† Electronic Supplementary Information (ESI) available: Electronic absorption spectra of binding of complexes **1-6** with DNA (Fig. S1), Electronic absorption titration of complexes **2-6** with EB bound to CT-DNA (Fig. S2), Cleavage of plasmid pBR322 DNA of complexes 1-6 and different incubation time at 37 °C (Fig. S3). Emission spectrum of BSA with compounds **2-6** (Fig. S4). CCDC numbers 1013683, 1013684, 1013685, 1013686, 1013687 and 1013688. For ESI and crystallographic data in CIF or other electronic format see DOI: 10.1039/b000000x/

compared to $CuCl_2$ and free $\mathbf{L^a}$, being 4-18 times more potent than cisplatin.[36,37]

on the other hand, Multitudinous studies showed that chiral complexes exhibited enantioselective binding or different binding constants to DNA compared with achiral metal complexes.[38-43] For Farukh Arjmand and his co-workers, a series of L-, D- and racemic LD-forms of the metal complexes based on diaminobenzene and tryptophan (L-, D-, LD-forms) was reported, in which the L-enantiomers of metal complexes showed more powerful binding ability to CT-DNA compared with D- or racemic complexes.[44] Similarly, Group Chew-Hee Ng reported two pairs of metal complexes [Cu(phen)(L/D-threo)(H_2O)]NO_3 (threo = threoninate) and L/D-[Cu(phen)(5MeOCA)(H_2O)]NO_3 (phen = 1,10-phenanthroline; 5MeOCA = 5-methyloxazolidine-4-carboxylate) to deduced that the the chirality of these ternary copper(II) complexes affects the DNA binding recognition .[45]

Previously, our group developed plenty of metal complexes containing polypyridyl ligands to bind with DNA.[46-48] For instance, three binuclear copper(II) complexes with 1,4-tpbd ligand (1,4-tpbd = N, N, N', N'-tetrakis(2-pyridylmethyl)benzene-1,4-diamine) showed effective oxidative DNA activity and possibly targeted DNA to inducing apoptosis in the selected cancer cell line.[47] With the goal of researching the significant bioactivity of polypyridyl ligands and chiral factor in complexes, we synthesized and characterized a series of copper(II) complexes derived from their respective achiral and chiral polypyridyl ligands ($\mathbf{L^1}$ and $\mathbf{L^{2(R/S)}}$) with naphthalene ring as a intercalating group for their probable bioactivities. All complexes were characterized by X-ray crystallography and their DNA cleavage properties and antitumour activity were investigated to verify their remarkable bioactivities and the influence of chirality.

Experimental

Materials and measurements

All reagents and chemicals were purchased from commercial sources and used as received. Ethidium bromide (EB), agarose, bovine serum albumin (BSA), calf thymus DNA (CT-DNA) and pBR322 plasmid DNA were obtain from Sigma. Tris-HCl buffer solution was prepared using deionized and sonicated triple-distilled water. Stock solutions of copper(II) complexes (1×10^{-3} M in acetonitrile) were stored at 4 °C and prepared to required concentrations for all experiments. Ultra-pure MilliQ water (18.24 MΩ cm) was used in all experiments. Human cervical carcinoma cell line (HeLa), human breast adenocarcinoma cell line (MCF-7) and Human endometrial carcinoma cell line (RL952) were obtained from the American Type Culture Collection (Rockville, MD, USA). Infrared spectra were recorded as KBr pellets on a BrukerVector 22 FT-IR spectrophotometer in the 4000-400 cm^{-1} regions. Electrospray ionization mass spectrometry (ESI-MS) was obtained on an Agilent 6520 Q-TOF LC/MS. The electronic spectral data were obtained on a JASCO V-570 spectrophotometer. The fluorescence spectra were measured on a MPF-4 fluorescence spectrophotometer at room temperature. The Gel Imaging and documentation DigiDoc-It System were assessed using Labworks Imaging and Analysis Software (UVI, UK). The circular dichroism (CD) spectra were taken on a JASCO-J715 spectropolarimeter. The MTT assay was revealed by measuring the absorbance of each well at 570 nm using a Bio-Rad 680 microplate reader (Bio-Rad, USA).

Synthesis of L^1•xHClO4, $L^{2(R/S)}$•xHClO4 (Scheme 1) and corresponding copper(II) complexes of 1-6

Synthesis of the tridentate polypyridyl ligand L^1•xHClO4.[49] 1-(chloromethyl)naphthalene (0.883 g, 5.00 mmol) in acetone (20 mL) was added dropwise to the mixture of di(2-picolyl)amine (1.003 g, 5.03 mmol) and K_2CO_3 (0.967 g, 7.00 mmol). After 25h reflux, the solvent was removed on a rotary evaporator. The residue was washed with water and then extracted several times with chloroform. The combined chloroform phases were washed three times with water then dried over $MgSO_4$ and the solvent was removed on a rotary evaporator. With the addition of perchlorate acid into ethanol solution (100 mL) of crude product, pale yellow precipitate was filtered and then recrystallized by ethanol (yield: 61%). FT-IR (KBr, ν, cm^{-1}): 1618, 1468, 1295, 1093, 801, 777, 731, 624.

Synthesis of the chiral enantiomers $L^{2(R/S)}$•xHClO4. The enantiomers were synthesized by the same method, except for the different chiral amine substrates.[50] An improvement was conducted based on the original method. Thus only the preparation for $\mathbf{L^{2(R)}}$ was described. NaOH (0.80 g, 20 mmol) was dissolved in water (34 mL) for the synthesis of $\mathbf{L^{2(R)}}$. 24 mL of the NaOH aqueous solution was added dropwise into 2.5 mL of ethanolic 2-picolyl chloride hydrochloride (1.48 g, 9.0 mmol). After the mixture turned into orange color, (R)-(+)-1-(1-Naphthyl) ethylamine (0.64 mL, 4 mmol) was added. NaOH aqueous solution (10 mL) was dripped into and the mixture was stirred in dark for a week at room temperate. Methylene chloride (3×20 mL) was added to extract the organic compounds and the organic layer was dried with anhydrous potassium carbonate. After the solvent was removed, the residues was dissolved in ethanol and precipitated with the addition of perchlorate acid, then recrystallized in ethanol (yield: 19%). FT-IR (KBr, ν, cm^{-1}): 1627, 1465, 1093, 760, 624.

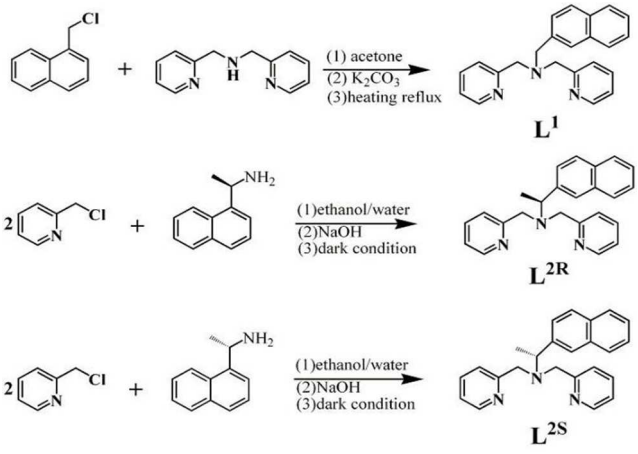

Scheme 1

Synthesis of copper(II) complexes 1-6. These complexes were similarly prepared. Complexes **1**, **3** and **4** were prepared from copper(II) chloride and complexes **2**, **5** and **6** were derived from copper(II) acetylacetonate (0.0425 g, 0.2 mmol). Thus a typical example was given for the preparation of [Cu$\mathbf{L^1}$Cl]ClO_4 (**1**). Copper(II) chloride (0.0270 g, 0.2 mmol) in ethanol (5 mL)

was added to a water-ethonal (1:1) mixture of **L^1•xHClO4** (0.1118 g, 0.2 mmol) and KPF_6 (0.0368 g, 0.2 mmol), followed by a few drop of LiOH aqueous solution until the pH of the solutions became ca. 7. The resulting dark blue solution was stirred for 3h at room temperature. Blue block crystals suitable for X-ray diffraction were obtained by slow evaporation of the filtrate for several days, which were washed with diethyl ether and dried in air after collected by filtration. [CuL^1Cl]ClO_4 (1)**:** yield: 53%. FT-IR (KBr, *v*, cm^{-1}): 1638, 1482, 1119, 619. ESI-MS (*m/z* = 447.10, [CuL^1(CH_3CH_2OH)-H]$^+$). [CuL^1(acac)]PF_6 **(2):** yield: 55%. FT-IR (KBr, *v*, cm^{-1}): 1637, 1401, 1118, 615. ESI-MS (*m/z* = 447.10, [CuL^1(CH_3CH_2OH)-H]$^+$). [Cu$L^{2(R)}$Cl]$_2(PF_6)_2$ (**3**)**:** yield: 38%. FT-IR (KBr, *v*, cm^{-1}): 1637, 1445, 1107, 844, 619. ESI-MS(*m/z* = 461.12, [Cu$L^{2(R)}$(CH_3CH_2OH)-H]$^+$). [Cu$L^{2(S)}$Cl]$_2(PF_6)_2$ **(4):** yield: 42%. FT-IR (KBr, *v*, cm^{-1}): 1642, 1117, 610. ESI-MS (*m/z* = 461.12, [Cu$L^{2(S)}$(CH_3CH_2OH)-H]$^+$). [Cu$L^{2(R)}$(acac)]PF_6 **(5):** yield: 28%. FT-IR (KBr, *v*, cm^{-1}): 1637, 1520, 1396, 1113, 842, 557. ESI-MS (*m/z* = 461.12, [Cu$L^{2(R)}$(CH_3CH_2OH)-H]$^+$). [Cu$L^{2(S)}$(acac)]PF_6 **(6):** yield: 41%. FT-IR (KBr, *v*, cm^{-1}): 1638, 1519, 1387, 1113, 842, 558. ESI-MS (*m/z* = 461.12, [Cu$L^{2(S)}$(CH_3CH_2OH)-H]$^+$).

Circular dichroism

Circular dichroism (CD) had become a versatile tool for studying chirality of metal complexes because of their difference in absorbance. All data of the two pairs of chiral enantiomers were taken on a JASCO-J715 spectropolarimeter at room temperature from 400 to 250 nm.

X-ray crystallography

Single-crystal X-ray diffraction data of complexes **1-6** were obtained at 113(2) K on a Bruker Smart 1000 CCD diffractometer using *Mo-Kα* radiation with the *ω* scan technique. The structures were solved by direct methods (SHELXS-97) and refined with full-matrix least-squares technique on F^2 using the SHELXL-97.[51] The hydrogen atoms were added theoretically, and riding on the concerned atoms and refined with fixed thermal factors. Crystallographic data for **1-6** had been deposited at the Cambridge Crystallographic Data Centre (CCDC) with CCDC numbers of 1013683, 1013684, 1013685, 1013686, 1013687 and 1013688, respectively.

DNA-binding experiments

Absorption spectrophotometric studies

The radio of 1.8-1.9 which was calculated by the UV absorbance at 260 nm and 280 nm of CT-DNA solution in 5 mM Tris–HCl/50 mM NaCl buffer (pH 7.2) indicated that DNA was sufficiently free of protein. Absorption spectra titrations were performed at room temperature in Tris/NaCl buffer (5 mM Tris–HCl/50 mM NaCl buffer, pH 7.2) to investigate the binding affinity between CT-DNA and complexes. 2 mL solution of the blank Tris/NaCl buffer and the copper(II) complex sample ([complex] = 1×10^{-3} M in acetonitrile) were placed into two 1 cm path cuvettes respectively. Then one aliquot (10 μL) of buffered CT-DNA solution (0.01 M) was added to each cuvette in order to eliminate the absorbance of DNA itself. Before the absorption spectra were recorded, the Cu(II)-DNA solutions were incubated at room temperature for 5 min in order to fully react.

Competitive binding experiments

The relative binding of complexes to CT-DNA was determined with an EB-bound CT-DNA solution in Tris/NaCl buffer (5 mM Tris–HCl/50 mM NaCl buffer, pH 7.2). The experiment was carried out by titrating a certain volume of a stock complex into EB–DNA solution containing 2.4 μM EB and 48 μM CT-DNA. The influence of the addition of complexes to the EB-DNA complex had been obtained by recording the variation of fluorescence emission spectra with excitation at 510 nm and emission at 602 nm. Before the emission spectra were recorded, the systems were incubated at room temperature for 5 min in order to fully react.

DNA cleavage and mechanism studies

The DNA cleavage experiments were done by agarose gel electrophoresis, which were performed by incubation at 37 °C as follows: pBR322 DNA (0.1 μg/μL) in 50 mM Tris-HCl/18 mM NaCl buffer (pH = 7.2) was treated with complexes **1-6** respectively. Different concentrations of complex were added to pBR322 DNA stock. The samples were incubated for 3h before the loading buffer was added in. Then the samples were electrophoresed for 2h in 0.9% agarose gel using Tris-boric acid-EDTA buffer. After electrophoresis, bands were visualized by UV light and photographed.

Cleavage mechanistic investigation of pBR322 DNA was carried out in the presence of relevant radical scavengers and reaction inhibitors. The reactions were conducted by adding standard radical scavengers of KI, NaN_3, L-histidine, SOD, EDTA and the groove binding agent Methyl Green (for major groove), SYBR Green (for minor groove) to pBR322 DNA before the addition of complexes. Cleavage was initiated by the addition of complexes and quenched with 2 μL of loading buffer. Further analysis was carried out by the above standard method.

Protein binding studies

The protein binding study was performed by fluorescence quenching experiments using bovine serum albumin stock solution (BSA, 1.5 mM) in 10 mM phosphate buffer (pH = 7.0). The fluorescence spectra were recorded at room temperature with an excitation wavelength of BSA at 280 nm and the emission at 342 nm by keeping the concentration of BSA constant (30 μM) while increasing the complex concentration regularly. In addition, absorption titration experiments were carried out by keeping the concentration of complexes (10 μM) and the BSA concentration (15 μM) constant.

MTT assay

A density of 2×10^3 cells per well in 100 μL medium was seeded in 96-well microassay culture plates (Costar) and then incubated for 48h at 37 °C and 5% CO_2. The cells were subsequently treated with different concentrations of complexes **1-6** for 72h. Then each well was loaded with 0.1 mg of MTT (in 20 μL of PBS, pH = 7.4). After 4h of incubation at 37 °C, a volume of 100 μL DMSO was added to dissolve the formed formazan crystals and the absorbance was read at 570 nm on a Biotek Microplate Reader. Experiments were carried out in triplicate, and IC_{50} values were calculated from plots of cell viability against dose of compound added.

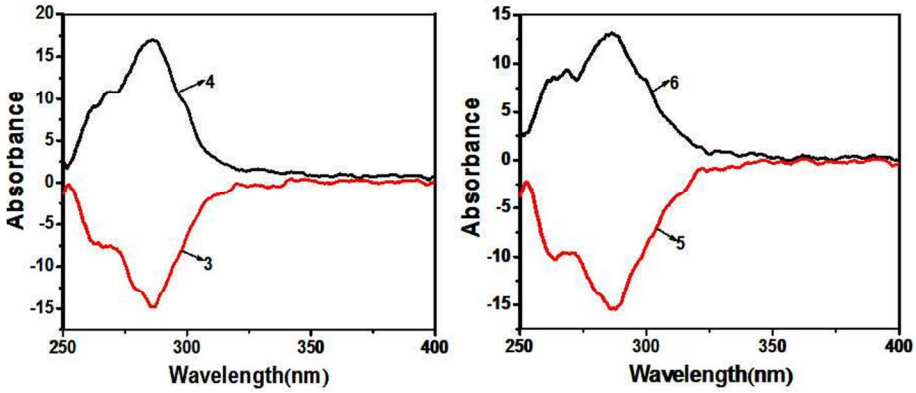

Fig. 1 The CD spectra of chiral complexes **3-6** in the acetonitrile solution

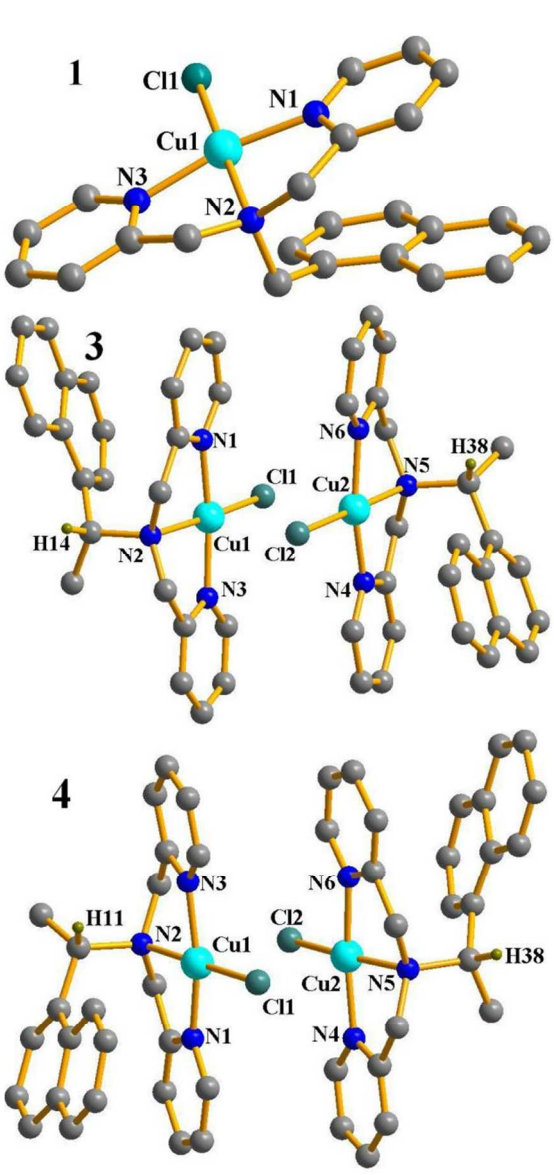

Fig. 2 Molecular structures of complexes **1, 3-4**; dissociative small molecules and non-essential H atoms are omitted for clarity.

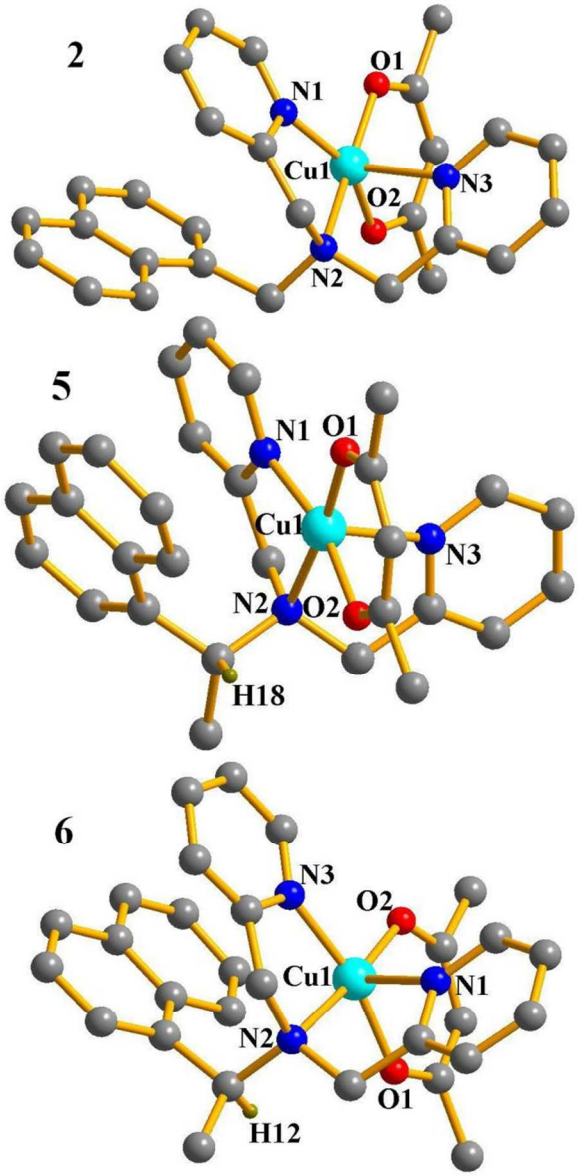

Fig. 3 Molecular structures of complexes **2, 5-6**; dissociative small molecules and non-essential H atoms are omitted for clarity.

Table 1 Crystallographic datas for complexes **1-6**.

Compound reference	**1**	**2**	**3**	**4**	**5**	**6**
Chemical formula	$C_{23}H_{21}Cl_2CuN_3O_4$	$C_{28}H_{28}CuF_6N_3O_2P$	$C_{48}H_{46}Cl_2Cu_2F_{12}N_6P_2$	$C_{48}H_{46}Cl_2Cu_2F1_2N_6P_2$	$C_{29}H_{30}CuF_6N_3O_2P$	$C_{29}H_{30}CuF_6N_3O_2P$
Formula Mass	537.87	647.04	1194.83	1194.83	661.07	661.07
Crystal system	Orthorhombic	Monoclinic	Orthorhombic	Orthorhombic	Orthorhombic	Orthorhombic
a/Å	13.966(4)	16.570(3)	14.286(3)	14.258(3)	12.0797(2)	11.948(3)
b/Å	13.887(4)	12.324(3)	15.106(3)	15.075(3)	14.2249(3)	14.110(3)
c/Å	23.249(6)	14.080(3)	23.050(5)	23.007(5)	17.4935(3)	17.229(4)
α/°	90.00	90.00	90.00	90.00	90.00	90.00
β/°	90.00	101.64(3)	90.00	90.00	90.00	90.00
γ/°	90.00	90.00	90.00	90.00	90.00	90.00
Unit cell volume/Å^3	4509(2)	2816.2(10)	4974.3(18)	4945.1(18)	3005.95(10)	2904.6(11)
Temperature/K	113(2)	113(2)	113(2)	113(2)	113(2)	113(2)
Space group	*Pbca*	*P2(1)/c*	*P2(1)2(1)2(1)*	*P2(1)2(1)2(1)*	*P2(1)2(1)2(1)*	*P2(1)2(1)2(1)*
Z	8	4	4	4	4	4
No. of reflections measured	33352	22877	36824	40815	7880	22145
No. of independent reflections	3976	4958	8749	8706	4809	5115
R_{int}	0.0468	0.0340	0.0416	0.0502	0.0169	0.0452
Final R_1 values ($I > 2\sigma(I)$)	0.0375	0.0305	0.0468	0.0485	0.0389	0.0387
Final $wR(F^2)$ values ($I > 2\sigma(I)$)	0.0982	0.0766	0.1197	0.1180	0.1071	0.0912
Final R_1 values (all data)	0.0407	0.0350	0.0506	0.0533	0.0428	0.0411
Final $wR(F^2)$ values (all data)	0.1007	0.0788	0.1232	0.1214	0.1129	0.0936
Goodness of fit on F^2	1.108	1.053	1.040	1.026	0.760	0.738

Table 2 Selected bond lengths (Å) and angles (º) for the complexes **1-6**.

Complex **1**							
Cu(1)-N(1)	1.981(2)	Cu(1)-N(3)	1.986(2)	Cu(1)-N(2)	2.042(2)	Cu(1)-Cl(1)	2.2522(9)
N(1)-Cu(1)-N(3)	165.78(9)	N(1)-Cu(1)-N(2)	83.51(8)	N(3)-Cu(1)-N(2)	82.27(8)	N(1)-Cu(1)-Cl(1)	96.85(6)
N(3)-Cu(1)-Cl(1)	97.34(7)	N(2)-Cu(1)-Cl(1)	173.76(6)				
Complex **2**							
Cu(1)-O(2)	1.9169(13)	Cu(1)-O(1)	1.929(13)	Cu(1)-N(1)	1.984(15)	Cu(1)-N(2)	2.073(15)
Cu(1)-N(3)	2.2338(18)	O(2)-Cu(1)-O(1)	94.46(6)	O(2)-Cu(1)-N(1)	154.29(6)	O(1)-Cu(1)-N(1)	93.81(6)
O(2)-Cu(1)-N(2)	89.59(6)	O(1)-Cu(1)-N(2)	175.03(6)	N(1)-Cu(1)-N(2)	83.71(6)	O(2)-Cu(1)-N(3)	97.14(6)
O(1)-Cu(1)-N(3)	98.34(6)	N(1)-Cu(1)-N(3)	105.68(6)	N(2)-Cu(1)-N(3)	78.27(6)		
Complex **3**							
Cl(1)-Cu(1)	2.2472(12)	N(1)-Cu(1)	1.988(3)	N(2)-Cu(1)	2.056(3)	N(3)-Cu(1)	1.983(3)
N(3)-Cu(1)-N(1)	166.55(15)	N(3)-Cu(1)-N(2)	82.82(15)	N(1)-Cu(1)-N(2)	84.42(15)	N(3)-Cu(1)-Cl(1)	96.73(12)
N(1)-Cu(1)-Cl(1)	96.49(12)	N(2)-Cu(1)-Cl(1)	172.26(10)	Cu(2)-N(4)	1.956(3)	Cu(2)-N(6)	1.985(3)
Cu(2)-N(5)	2.069(3)	Cu(2)-Cl(2)	2.260(11)	N(4)-Cu(2)-N(6)	166.1(14)	N(4)-Cu(2)-N(5)	83.27(14)
N(6)-Cu(2)-N(5)	82.82(15)	N(4)-Cu(2)-Cl(2)	97.62(11)	N(6)-Cu(2)-Cl(2)	96.28(11)	N(5)-Cu(2)-Cl(2)	179.01(10)
Complex **4**							
Cu(1)-N(1)	1.950(4)	Cu(1)-N(2)	1.961(3)	Cu(1)-N(3)	1.976(4)	Cu(1)-Cl(1)	2.1431(11)

N(1)-Cu(1)-N(2)	83.66(15)	N(1)-Cu(1)-N(3)	166.98(14)	N(2)-Cu(1)-N(3)	83.39(16)	N(1)-Cu(1)-Cl(1)	97.21(12)
N(2)-Cu(1)-Cl(1)	178.97(12)	N(3)-Cu(1)-Cl(1)	95.72(12)	Cu(2)-N(4)	1.974(4)	Cu(2)-N(5)	1.931(3)
Cu(2)-N(6)	1.978(4)	Cu(2)-Cl(2)	2.1358(12)	N(5)-Cu(2)-N(4)	83.33(16)	N(5)-Cu(2)-N(6)	84.48(16)
N(4)-Cu(2)-N(6)	166.98(15)	N(5)-Cu(2)-Cl(2)	171.52(11)	N(4)-Cu(2)-Cl(2)	96.18(12)	N(6)-Cu(2)-Cl(2)	96.55(12)
Complex **5**							
Cu(1)-O(2)	1.924(3)	Cu(1)-O(1)	1.932(3)	Cu(1)-N(1)	1.989(3)	Cu(1)-N(2)	2.106(3)
Cu(1)-N(3)	2.226(4)	O(2)-Cu(1)-O(1)	93.34(12)	O(2)-Cu(1)-N(1)	166.2(13)	O(1)-Cu(1)-N(1)	94.01(12)
O(2)-Cu(1)-N(2)	88.43(12)	O(1)-Cu(1)-N(2)	173.59(12)	N(1)-Cu(1)-N(2)	83.05(12)	O(2)-Cu(1)-N(3)	91.50(13)
O(1)-Cu(1)-N(3)	108.52(12)	N(1)-Cu(1)-N(3)	97.26(12)	N(2)-Cu(1)-N(3)	77.56(12)		
Complex **6**							
Cu(1)-O(1)	1.921(3)	Cu(1)-O(2)	1.929(2)	Cu(1)-N(3)	1.987(3)	Cu(1)-N(2)	2.103(3)
Cu(1)-N(1)	2.232(3)	O(1)-Cu(1)-O(2)	93.99(10)	O(1)-Cu(1)-N(3)	166.4(12)	O(2)-Cu(1)-N(3)	93.54(11)
O(1)-Cu(1)-N(2)	87.70(10)	O(2)-Cu(1)-N(2)	173.75(11)	N(3)-Cu(1)-N(2)	83.66(11)	O(1)-Cu(1)-N(1)	91.42(11)
N(3)-Cu(1)-N(1)	96.97(11)	N(2)-Cu(1)-N(1)	77.96(11)				

Results and discussion

Circular dichroism

Circular dichroism was the differential absorbance of left minus right circularly polarized light. Thus, the sign of the obtained bands was characteristic of the absolute configuration of the molecule, and for chiral transition metal complexes, these bands could be either ligand transitions or d-d transitions of the metal ion.[52] The CD spectra of the two enantiomeric couples, namely **(3)/(4)** and **(5)/(6)** showed the expected mirror-image relationship (Fig. 1) in acetonitrile. The two chiral enantiomers emited the equal intense peak with the opposite orientation, respectively, which demonstrated the correctness of the existence of two chiral enantiomers. Complexes **3** and **5** were characterized by the following CD bands indicative of the *R* ligand configuration (band wavelength, sign and strength were indicated): ca. 284(–, medium). The same trends of S-enantiomers could also be found in Fig. 1.

X-ray structure characterization

The single crystal X-ray analysis revealed that these complexes could be grouped into two categories for the different coordination configuration. The copper centers of **1**, **3** and **4** were distorted square planar which were showed in Fig. 2, while the copper centers of **2**, **5** and **6** were square pyramid due to the different coordinated anion which exhibited in Fig. 3. The details of crystallographic data and structure refinement parameters of these complexes were summarized in Table 1. Selected bond angles and distances were listed in Table 2.

The crystal systems of **1**, **3** and **4** were orthogonal with the space group of *pbca* (**1**) and *P212121* (**3** and **4**). The structures of three compounds consisted of mononuclear $[CuLCl]^+$ cations and ClO^{4-} (**1**) or PF^{6-} (**3** and **4**) counterions. Significantly, the asymmetric unit of **3** and **4** were comprised of two similar mononuclear $[CuL^2Cl]^+$ species with the intermolecular Cu1-Cl2 and Cu2-Cl1 distances of 2.832 Å, 2.910 Å (**3**) and 3.066 Å, 2.985 Å (**4**). The copper(II) centers all had square planar geometry consisting of N_3Cl donor set, which were two pyridine N atoms (N_{Py}), one tertiary amine N atom (N_{am}) and one coordinated Cl atom. Deviation of the copper ion from the least-squares plane were only 0.0699 Å (**1**), 0.0106 Å (**3**) and 0.0130 Å (**4**), respectively, testifying the square planar coordination structure of the three complexes in Fig. 2. Compared with the approximate verticality of benzene and pyridine (dihedral angel 89.729°) in a reported similar complex of $[Cu^{II}L'(Cl)]ClO_4$ (**L'** = N,N-Di(2-pyridylmethyl)-2-phenylethylamine)[53],naphthaline ring and the pyridine ring were approximate parallel as the dihedral angels were 17.904° (**1**), 18.016° (**2**) and 18.504° (**3**).

Complex **2** was crystallized in monoclinal space group of *P2(1)/c*, while the space group of chiral enantiomers **5** and **6** were P212121. In **2**, **5** and **6**, a bidentate acac ligand replaced the monodentate Cl anion in **1**, **3** and **4**, thus each copper(II) centers were N_3O_2 five-coordinated with distorted square-pyramidal geometry (Fig. 3). The geometry was attested by the corresponding τ values (τ = 0.35, 0.124 and 0.122 for **2**, **5** and **6**) in according to addison-reedijk geometry standard.[54] Two O atoms of acac, one N_{Py} and one N_{am} share the base-to-apex edges so that the final N_{Py} situates at the vertex of the distorted square pyramid structure with longer Cu-N distance of 2.2338 Å (**2**), 2.226 Å(**5**) and 2.232 Å (**6**). Also the small dihedral angels 27.142° (**2**), 20.366° (**5**) and 19.534° (**6**) of naphthaline ring and the adjacent pyridine ring were calculated.

Electronic absorption titration

DNA binding was the critical process for DNA cleavage in many cases. As a significant binding model of complexes to DNA, intercalation usually resulted in hypochromism and bathochromism of the absorption intensity, involving strong stacking interaction between complexes and the base pairs of DNA. While Minor groove binding of complexes to DNA usually leaded to hyperchromism in absorption intensity, indicating the unwinding of the DNA double helix as well as its unstacking and the concomitant exposure of the bases.[55-57]

Considered as a basic testing method, electronic absorption

Table 3 DNA and BSA binding constants of complexes **1- 6**.

Complex	$\Delta\varepsilon$(%)	K_b (M^{-1})	K_{app} (M^{-1})	K_{sv}(M^{-1})	K_q(M^{-1})	n
1	17.15	8.68×10^5	2.08×10^5	1.19×10^4	2.08×10^4	1.0
2	14.76	4.97×10^5	2.15×10^5	1.70×10^4	1.53×10^4	0.99
3(R)	10.09	5.87×10^5	1.24×10^5	1.25×10^4	2.03×10^4	1.10
4(S)	21.52	1.73×10^6	1.26×10^5	1.33×10^4	1.28×10^5	1.25
5(R)	7.98	1.15×10^6	2.09×10^5	1.42×10^4	1.59×10^4	1.01
6(S)	14.63	3.46×10^6	2.18×10^5	1.66×10^4	1.06×10^4	0.96

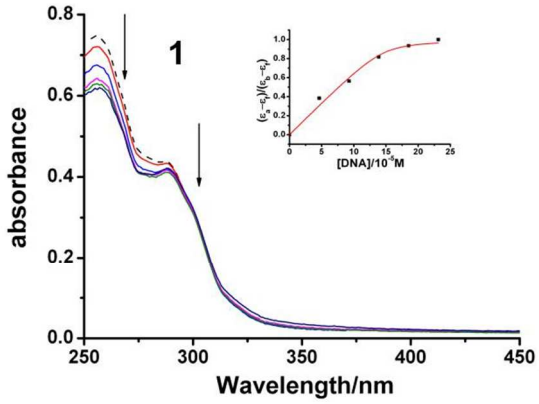

Fig. 4 Absorption spectra of complex **1** (50 μM) in the absence (dashed line) and presence (solid line) of increasing amounts of CT-DNA at room temperature in 5mM Tris–HCl/50mM NaCl buffer (pH= 7.2). The arrow shows the absorbance changes on increasing CT-DNA concentration. Inset shows the plot of $(\varepsilon_a-\varepsilon_f)/(\varepsilon_b-\varepsilon_f)$ vs. [DNA].

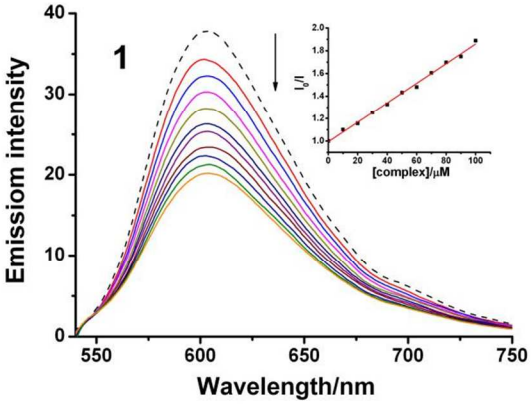

Fig. 5 Effect of addition complex 1 on the emission intensity of EB bound to CT-DNA at different concentrations in 5Mm Tris–HCl/50mM NaCl buffer (pH 7.2), inset: plot of I_0/I vs. [complex].

spectroscopy was one of the most common techniques in examining the binding mode of DNA with the metal complexes. Therefore, the typical titration curve for the complexes in the absence and presence of CT-DNA at different concentrations were implemented and the results were showed in Fig. 4 and Fig. S1.

In the UV spectrum of complexes **1-6**, the similar bands of 255 to 257 nm were attributed to intraligand π–π* transition. Upon the incremental addition of CT-DNA, the bands of **1-6** exhibited significant hypochromism of 7.98%-21.52%. The results derived from the UV-Vis titration experiments suggested that all the complexes could bind to DNA via partial intercalation, because intercalation would lead to hypochromism in UV absorption spectra due to the intercalative mode involving a strong stacking interaction between an aromatic chromophore and the base pairs of DNA.[58] The intrinsic binding constants K_b reflecting binding strength of the complexes and CT-DNA were calculated according to the equation.[59,60]

$$(\varepsilon_a-\varepsilon_f)/(\varepsilon_b-\varepsilon_f)=\left(b-\left(b^2-2K_b{}^2C_t[DNA]/s\right)^{1/2}\right)/2K_bC_t \qquad (1a)$$

$$b=1+K_bC_t+K_b[DNA]/2s \qquad (1b)$$

Deduced by the equation, magnitude of the K_b values of six complexes were 10^5 and 10^6, and more details were showed in Table 3. According to reduction rate of $\Delta\varepsilon$ and the K_b values induced by these chiral complexes, the perturbation on the base-stacking of CT-DNA followed an order of **3(R)<4(S)**, **5(R)<6(S)**. Little difference between the chiral enantiomers may due to the tiny variation of chiral methyl in ligands. Compared with the K_b values (10^4 magnitude) of similar copper(II) complexes which were reported by Zi-Jian Guo group[61], the minimum K_b value of the six copper complexes was 4.97×10^5, which indicated more efficient DNA binding activity due to the intercalation of naphthaline ring with the base pairs of DNA.

Fluorescence spectroscopy

Fluorescence spectral technique was an effective method to study the interaction of metal complex with DNA. Hence a fluorescence-quenching experiments with EB-bound DNA was undertaken to understand the mode of DNA interaction with the copper(II) complexes. The molecular fluorophore EB emited intense fluorescence at about 600 nm in the presence of DNA due to its strong intercalation between adjacent DNA base pairs.[62] Addition of a second molecule, which bound to DNA more strongly than EB, would displace bound EB and quenched the DNA-induced EB emission.[63] The extent of quenching of the fluorescenc of EB bound to DNA would reflect the extent of DNA binding of the second molecule.

Aliquots of the complexes solution were then added to the EB-

DNA solution in 5 mM Tris–HCl/50 mM NaCl buffer (pH= 7. 2), and the fluorescence was measured after each addition until a 50% reduction of fluorescence appeared. Fluorescence intensities were measured at room temperature (λex = 510 nm; λem = 602 nm) and showed in Fig. 5. The apparent binding constants (K_{app}) of the complexes were calculated using the equation

$$K_{EB}[\mathrm{EB}] = K_{app}[\mathrm{complex}]$$

where the complex concentration was the value at a 50% reduction of the fluorescence intensity of EB, and K_{EB}= 1.0×10^7 M^{-1} ([EB] = 2.4 μM), typical of classical intercalators and metallo-intercalators with K of the order of 107 M-1.64 The apparent binding constants (K_{app}) at room temperature were calculated to 10^5 magnitude, which indicated that the interaction of the complexes with DNA were moderate intercalative mode. More detailed values were also showed in Table 3. With the similar tridentate ligand, Pramod and his co-workers studied the ability of complex $[Cu(Pyimpy)(Cl)_2]\cdot 2H_2O$ (Pyimpy = (2-((2-phenyl-2-(pyridin-2-l)hydrazono)methyl) pyridine)) to bind with DNA via fluorescence spectral technique, as the apparent binding constant (K_{app}) was 7.33×10^4,[65] which was much less than the value of the six complexes. The reason may be the naphthalene ring of the six complexes could intercalate into the base pairs of DNA more efficiently when compared with benzene ring.[66,67] On the basis of the titration profiles, K_{app} of complexes **3-6** was calculated as 1.24×10^5, 1.26×10^5, 2.09×10^5, 2.18×10^5, respectively. The results were in accordance with the above electronic absorption titration observations.

The cleavage of pBR322 DNA

The DNA cleavage activity of the complexes was studied using supercoiled pBR322 plasmid DNA by gel electrophoresis in the buffer (50 mM Tris–HCl/18 mM NaCl, pH = 7.2) in the absence of external agents under physiologically relevant conditions. Fig. 6 showed the treatment of pBR322 DNA with different concentrations of all complexes in the presence of H_2O_2 (0.25 mM). The chiral complexes could convert the Form I DNA into Form II and little Form III thoroughly at 20 μM (lane 3) while the achiral complexes were at 35 μM (lane 4), which indicated the better cleavage activity of chiral complexes. And also dependency on concentration of complexes could be deduced by Fig. 6. The similar copper complex $[Cu\mathbf{L}^xCl_2]\cdot H_2O$ ($\mathbf{L}^x$ = (2-pyridin-2-ylethyl)pyridin-2-ylmethyleneamine) with a tridentate polypyridyl ligand could only convert 50% Form I DNA into Form II, which was much inferior than complexes **1-6**. The probable reason may be the intercalation of naphthalene ring in **1-6** and DNA base pairs promoted the DNA damage process.

The time-dependent cleavage of DNA by the six complexes was also studied under similar conditions. With increased reaction time, the amounts of Forms II and III increased and Form I gradually disappeared. The results show that cleavage of DNA by the two complexes was dependent on reaction time (shown in Fig. S3).

DNA cleavage mechanism

In order to identify that the ROS were responsible for the DNA cleavage reaction, we continued to explore the influence of different potentially inhibiting agents including hydrogen radical scavenger (KI), singlet oxygen quenchers (NaN_3), superoxide scavenger (SOD, superoxide dismutase), peroxide anion scavenger (catalase) and chelating agent (EDTA) under our experimental conditions.[69] No obvious inhibition was discovered

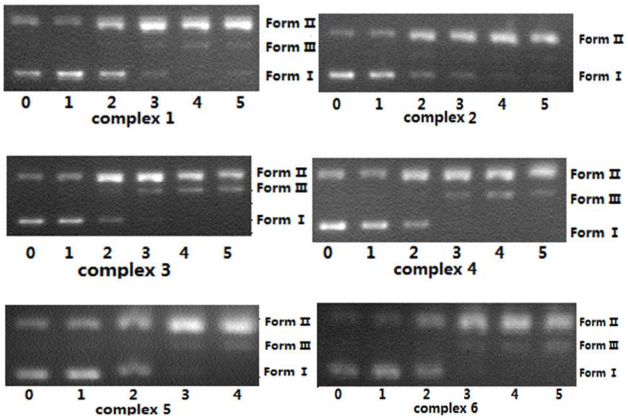

Fig. 6 Cleavage of plasmid pBR322 DNA (0.1 μg/μL) with different concentrations of complexes **1-6** after 3h incubation at 37 °C. Lane 0, DNA control; lane 1, DNA + H_2O_2 (0.25 mM); lane 2~5, DNA + H_2O_2 (0.25 mM) + complex (5, 20, 35, 50 μM), respectively.

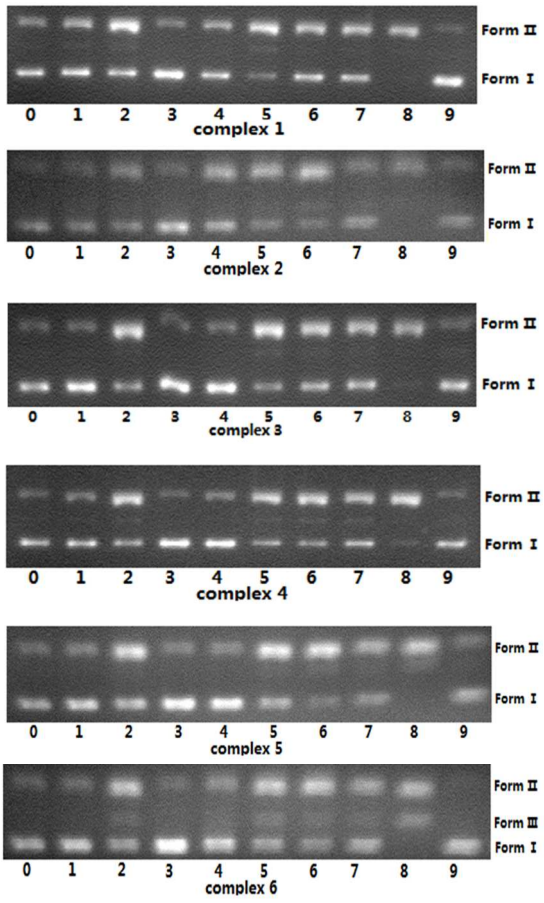

Fig. 7 Cleavage of plasmid pBR322 DNA (0.1 μg/μL) in the presence of 5 μM complexes **1-6** and different inhibitors after 3h incubation at 37 °C. For complexes **1-6**, lane 0, DNA control; Lane 1, DNA + H_2O_2 (0.25mM); Lane 2, DNA + H_2O_2 (0.25 mM) + complex (5 μM); Lane 3-9, DNA + H_2O_2 (0.25 mM) + complex (5 μM) + inhibitors (20 mM KI, 20 mM NaN_3, 20 U/mL SOD, 20 U/mL catalase, 10 U/mL SYBR Green, 0.1 mM methyl green, 20 mM EDTA).

for complexes in the presence of SOD (lane 5) and catalase (lane 6) in Fig. 8, which ruled out the possibility of DNA cleavage by superoxide and peroxide anion. KI markedly inhibited the cleavage activity of the complexes (lane 3 of all), suggesting that hydrogen radicals were involved in the cleavage reaction. NaN_3 significantly diminishes the cleavage activity of the complexes (lane 4 of all), suggesting that $^1O_2$ also took part in the cleavage mechanism. The phenomenon that the chelating agent EDTA (lane 9) had the ability to efficiently inhibit DNA cleavage manifested Cu^{2+} played a key role in the DNA cleavage. In order to assure the sites of interaction between the complexes and DNA, the SYBR Green (lane 7) and methyl green (lane 8) were added, which were known to interact to DNA at minor and major grooves. The result that the addition of methyl green could accelerate DNA cleavage while SYBR Green hadn't suggested the complexes preferred to bind to DNA major groove. In summary, these complexes followed similar pathways in the cleavage process, in which hydroxyl radical and singlet oxygen were crucial ROS for the cleavage reactions.

Protein binding studies

Bovine serum albumin (BSA) was the most extensively studied serum albumin, due to its structural homology. For the two intrinsic characteristics of the protein, namely tryptophan and tyrosine, a remarkable fluorescence of BSA was observed.[70] And protein conformational transitions, subunit associations, substrate binding, or denaturation could cause the changes in the emission spectra of tryptophan. Thus the intrinsic fluorescence of BSA provided considerable information on their structure and was often utilized in the study of protein folding and association reactions.[71] Fig. 8 showed the effect of increasing the concentration of added complex **1** on the fluorescence emission of BSA (similar spectra of complexes **2-6** were presented in Fig. S4). The intensity of the characteristic broad emission band at 342 nm decreases regularly with the increasing concentration of complexes, which confirmed that the interaction between complexes and BSA had occurred.

The fluorescence quenching constant K_{sv} could be calculated by the Stern-Volmer equation ($I_0/I = 1 + K_{sv}[Q]$), where I_0 and I were the fluorescence intensities of the fluorophore in the absence and presence of a quencher, respectively. With the addition of complexes, the fluorescence intensity reduced significantly, which proved the interaction of complex with BSA. And the binding constants could be analyzed according to the Scatchard equation,

$$\log[(I_0 - I)/I] = \log K_q + n \log[Q]$$

where K_q was the binding constant of the complexes with BSA and n was the number of binding sites (shown in Table 3). The calculated value of n was around 1, indicating the existence of just a single binding site in BSA for all of the complexes.[72]

Quenching could occur by different mechanisms, which were usually classified as dynamic quenching and static quenching. Dynamic quenching referred to a process in which the fluorophore and the quencher came into contact during the transient existence of the excited state, while static quenching referred to fluorophore-quencher complex formation in the ground state. An effictive method to identify the type of quenching was UV-visible absorption spectroscopy. UV-visible (UV-Vis) spectra of BSA in the absence and presence of the compounds (Fig. 9) showed that the absorption intensity of BSA was enhanced as the complexes were added, and there was a little blue shift. It revealed that there existed a static interaction between BSA and the added complexes due to the formation of the ground state complex of the type of BSA-compound.[60]

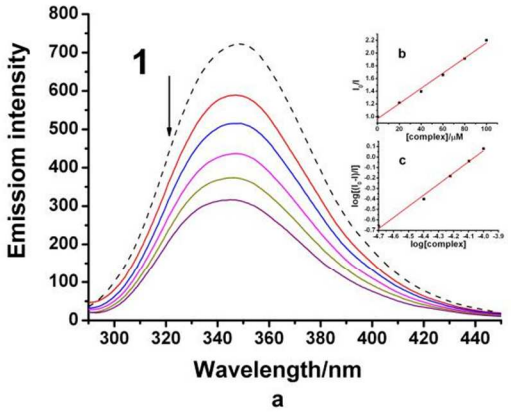

Fig. 8 The emission spectrum of BSA (30 μM; λexi = 290 nm; λemi = 345 nm) in the presence of increasing amounts of complex **1**. The dash line shows the intensity in the absence of complex. The arrow shows the fluorescence quenching upon increasing the concentrations of the complex (a). The inset shows the Stern–Volmer plots (b) and Scatchard plots (c) of the complex with BSA.

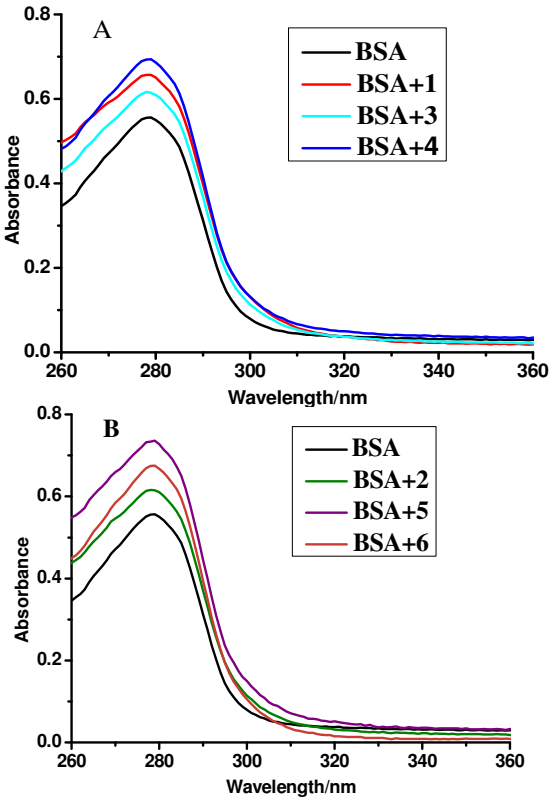

Fig. 9 Absorption spectra of BSA (15 μM) in the buffer solution (Tris–HCl) in the absence and presence of complexes(10 μM) of complexes **1-6**.

Table 4 *In vitro* cytotoxicity assays for complexes **1-6**, cisplatin and carboplatin against different cancer cell lines.

Complex	IC_{50}/μM by MTT assay			
	HeLa	MCF-7	HepG-2	Bel-7404
1	8.114±1.209	17.473±0.654	7.523±0.256	10.037±0.741
2	7.944±0.207	24.448±1.784	9.244±0.211	8.351±0.445
3(R)	4.704±0.574	9.501±0.0741	4.925±0.334	3.587±0.124
4(S)	4.919±0.387	10.129±0.247	4.732±0.119	4.303±1.22
5(R)	5.511±0.204	10.521±0.415	6.840±0.052	5.902±0.359
6(S)	5.283±0.541	16.089±2.331	6.900±0.045	6.98±1.227
Cisplatin[38]	12.1±0.6	3.92±0.56	4.00±0.32	---
Carboplatin[74]	---	36.65±6.56	27.96±3.15	---

IC_{50} = is the concentration of drug required to inhibit the growth of 50% of the cancer cells (μM).

MTT assay

In order to understand the in vitro cytotoxicity of the metal complexes **1-6**, the experiments were carried out using a panel of cell lines namely HeLa (human cervical carcinoma), MCF-7 (human breast adenocarcinoma), Bel-7404 (human hepatocellular carcinoma) and HepG-2 (human hepatocellular carcinoma) by colorimetric (MTT) assay in which mitochondrial dehydrogenase activity was measured as an indication of cell viability. Cisplatin and carboplatin were used as standards to assess the cytotoxicity of complexes **1-6**.[59,73] The results of MTT assays revealed that complexes **1-6** showed notable activity against both the cell lines mentioned above with low IC_{50} values. For HeLa, the respective IC_{50} values of complexes **1-6** were 8.114, 7.944, 4.704, 4.919, 5.511, 5.283 μM, which indicated that the chiral enantiomers were similar and stronger in cytotoxicity, almost exhibiting approximately 3 times antitumor effect than cisplatin. For all four tumor cells, the chiral complexes **3-6** showed higher anticancer acitivity than achiral complexes **1-2,** indicating chirality could be a significant factor when designing efficient anti-cancer drugs. In general, the six complexes showed superior anti-tumor acitivity and chirality would enhanced the potency as expected.

Conclusion

This work described the synthesis and characterization of two achiral complex **1-2** and two chiral enantiomers complex **3-6** for the reason to research the influence of chirality when interacted with biomolecules. The copper cations in **1**, **3-4** were four-coordinated within N_3Cl donor sets tending towards distorted square planar. While the coordination environment of copper cations in **2**, **5-6** were square pyramid within five-coordinated N_3O_2 donor sets. The DNA binding properties were investigated by electronic absorption titration, EB-DNA displacement experiments. The results indicated that the complexes shared the same binding mode, namely partial intercalation binding to CT-DNA. The values of K_b and K_{app} elucidated that all complexes owned favorable binding ability to CT-DNA. The agarose gel electrophoresis experiments revealed that all complexes could cleave plasmid pBR322 DNA thoroughly in the presence of H_2O_2 on the concentration of 35 μM, which was confirmed to be the oxidative mechanism produced by hydroxyl radical or singlet oxygen. And chiral enantiomers exhibited better cleavage activity than achiral complexes. Obvious fluorenscence quenching could be observed when they binding with BSA and static quenching mechanism were certified by electronic absorption titration. Especially, the complexes showed effective extensive anti-tumor potency with low IC_{50} values tested by MTT assay. And the chiral complexes showed stronger cytotoxicity compared with the achiral complexes in four cancer cells mentioned above, which demonstrated the influence of chirality against tumour eventually.

Acknowledgements

This work was supported by the National Natural Science Foundation of China (21171101, 21071083 and 21471085), Tianjin Science Foundation (No.12JCYBJC13600), NFFTBS (No. J1103306) and MOE Innovation Team (IRT13022) of China.

References

1 F. Jacob and J. Monod, *J. Mol. Biol.*, 1961, **3**, 318.
2 J. C. Venter, M. D. Adams, E. W. Myers and P. W. Li, *Science*, 2001, **291**, 1304.
3 E. U. Selker, Annu. *Rev. Genet.*, 1990, **24**, 579.
4 K. Kobayashi, S. D. Ehrlich, A. Albertini, G. Amati and K. K. Andersen, *Proc. Natl. Acad. Sci.*, 2003, **100**, 4678.
5 J. J. Elser, R. W. Stemer, E. Gorolhova, W. F. Fagan, T. A. Markow, J. B. Cotner, J. F. Harrison, S. E. Hobbie, G. M. Odell and L. J. Weider, *Ecol. Lett.*, 2000, **3**, 540.
6 L. M. Coussens and Z. Werb, *Nature*, 2002, **420**, 860.
7 C. J. Sherr, *Science*, 1996, **274**, 1672.
8 H. Davies, G. R. Bignell, C. Cox, P. Stephens, S. Edkins, S. Clegg, J. Teague and H. Woffendin, *Nature*, 2002, **417**, 949.
9 C. J. Sherr and F. McCormick, *Nature*, 2002, **2**, 103.
10 P. Correa, W. Haensel, C. Cuello, S. Tannenbaum and M. Archer, *Lancet*, 1975, **2**, 58.
11 R. Siegel, D. Naishadham and A. Jemal, *Ca-cancer J. Clin.*, 2013, **63**, 11.
12 D. Hanahan and R. A. Weinberg, *Cell*, 2000, **100**, 57.
13 T. Reya, S. J. Morrison, M. F. Clarke and I. L. Weissman, *Nature*, 2001, **414**, 105.
14 D. Hanahan and Robert A. Weinberg, *Cell*, 2011, **144**, 646.
15 R. K. Jain, *Science*, 2005, **307**, 58.
16 L. H. Hartwell and M. B. Kastan, *Science*, 1994, **266**, 1821.
17 P. A. Jones and S. B. Baylin, *Cell*, 2007, **128**, 683.

18 L. Paleari, A. Grozio, A. Cesario and P. Russo, *Semin. Cancer Biol.*, 2008, **18**, 211.
19 E. R. Jamieson and S. J. Lippard, *Chem. Rev.*, 1999, **99**, 2467.
20 C. X. Zhang and S. J. Lippard, *Curr. Opin. Chem. Biol.*, 2003, **7**, 481.
21 P. C. Bruijnincx and P. J. Sadler, *Curr. Opin. Chem. Biol.*, 2008, **12**, 197.
22 B. Rosenberg and L. VanCamp, *Cancer Res.*, 1970, **30**, 1799.
23 P. J. Loehrer and L. H. Einhorn, *Ann. Intern. Med.*, 1984, **100**, 704.
24 J. H. Edmonson, L. M. Ryan, R. H. Blum, J. S. Brooks, M. Shiraki, S. Frytak and D. R. Parkinson, *J. Clin. Oncol.*, 1993, **11**, 1269.
25 K. Nooter and G. Stoter, *Path. Res. Pract.*, 1996, **192**, 768.
26 R. S. Go and A. A. Adjei, *J. Clin. Oncol.*, 1999, **17**, 409.
27 J. M. McCord and I. Fridovich, *J. Biol. Chem.*, 1969, **244**, 6049.
28 E. I. Solomon, P. Chen, M. Metz, S. K. Lee and A. E. Palmer, *Angew. Chem. Int. Ed.*, 2001, **40**, 4570.
29 C. Liu, M. Wang, T. Zhang and H. Sun, *Coord. Chem. Rev.*, 2004, **248**, 147.
30 J. He, P. Hu, Y. J. Wang, M. L. Tong, H. Sun, Z. W. Mao and L. N. Ji, *Dalton Trans.*, 2008, 3207.
31 C. Santini, M. Pellei, V. Gandin, M. Porchia and F. Tisato, *Chem. Rev.*, 2014, **114**, 815.
32 F. Arjmand and M. Aziz, *Eur. J. Med. Chem.*, 2009, **44**, 834.
33 M. Chauhan and F. Arjmand, *Chem. Biodivers.*, 2006, **3**, 660.
34 H. Wu, X. Huang, B. Liu, F. Kou and J. Yuan, *J. Coord. Chem.*, 2011, **64**, 4383.
35 R. Ruiz, B. García, J. G. Tojal, N. Busto, S. Ibeas, J. M. Leal, C. Martins, J. Gaspar, J. Borrás, R. G. García and M. G. Álvarez, *J. Biol. Inorg. Chem.*, 2010, **15**, 515.
36 K. Ghosh, P. Kumar, N. Tyagi, N. Goel and M. C. Baratto, *Polyhedron*, 2011, **30**, 2667.
37 C. Santin, M. Pellei, V. Gandin, M. Porchia, F. Tisato and C. Marzano, *Chem. Rev.*, 2014, **114**, 815.
38 S. Satyanarayana, J. C. Dabrowiak and J. B. Chaires, *Biochemistry*, 1993, **32**, 2573.
39 A. K. Patra, T. Bhowmick, S. Ramakumar and A. R. Chakravarty, *Inorg. Chem.*, 2007, **46**, 9030.
40 V. Rajendiran, M. Murali, E. Suresh, M. Palaniandavar, V. S. Periasamy and M. A. Akbarsha, *Dalton Trans.*, 2008, 2157.
41 Y. Wu, H. Chen, P. Yang and Z. Xiong, *J. Inorg. Biochem.*, 2005, **99**, 1126.
42 F. Gao, H. Chao, F. Zhou, X. Chen, Y.-F. Wei and L.-N. Ji, *J. Inorg. Biochem.*, 2008, **102**, 1050.
43 C. H. Ng, W. S. Wang, K. V. Chong, Y. F. Win and K. E. Neo, *Dalton Trans.*, 2013, **42,** 10233
44 F. Arjmand, M. Muddassir and R. H. Khan, *Eur. J. Med. Chem.*, 2010, **45**, 3549.
45 C. H. Ng, W. S. Wang, K. V. Chong, Y. F. Win and K. E. Neo, *Dalton Trans.*, 2013, **42**, 10233.
46 J. Qian, L. Wang, W. Gu, X. Liu, J. L. Tian and S. P. Yan, *Dalton Trans.*, 2011, **40**, 5617.
47 D. D. Li, J. L. Tian, W. Gu, X. Liu, H. H. Zeng and S. P. Yan, *J.Inorg. Biochem.*, 2011, **105**, 894.
48 D.D. Li, J. L. Tian, Y. Y. Kou, F. P. Huang, G. J. Chen, W. Gu, X. Liu, D. Z. Liao, P. Cheng and S. P. Yan, *Dalton Trans.*, 2009, **18**, 3574.
49 L. Götzke, K. Gloe, K. A. Jolliffe, L. F. Lindoy, A. Heine, T. Doert and A. Jäger, *Polyhedron*, 2011, **30**, 708.
50 J. Zhang, A. E. Holmes, A. Sharma, N. R. Brooks, R. S. Rarig, J. Zubieta and J. W. Canary, *Chirality*, 2003, **15**, 180.
51 G. Sheldrick, *Acta Crystallogr., Sect. A: Found. Crystallogr.*, 2008, **64**, 112.
52 M. Enamullah, A. K. M. R. Uddin, G. Pescitelli, R. Berardozzi, G. Makhloufi, V. Vasylyeva, A. C. Chamayou and C. Janiak, *Dalton Trans.*, 2014, **43**, 3313.
53 T. Osako, Y.i Ueno, Y. Tachi and S. Itoh, *Inorg. Chem.*, 2003, **24**, 8087
54 A. W. Addison, T. N. Rao, R. J. J. V. Rijn and G. C. Verschoor, *J. Chem. Soc. Dalton Trans.*, 1984, 1349.
55 P. Kumar, S. Gorai, M. K. Santra, B. Mondal and D. Manna, *Dalton Trans.*, 2012, **41**, 7573.
56 F. Mancin, P. Scrimin, P. Tecilla and U. Tonellato, *Chem. Commun.*, 2005, 2540.
57 L. Tjioe, A. Meininger, T. Joshi, L. Spiccia and B. Graham, *Inorg. Chem.*, 2011, **50**, 4327.
58 F. Arjmand, M. Muddassir and I. Yousuf, *J. Photochem. Photobiol.*, B, 2014, **136**, 62-71.
59 D. S. Raja, N. S. P. Bhuvanesh and K. Natarajan, *Inorg. Chem.*, 2011, **50**, 12852.
60 Y. J. Hu, Y. Ou-Yang, C.M. Dai, Y. Liu and X. H. Xiao, *Biomacromolecules*, 2010, **11**, 106.
61 X. Dong, X. Wang, M. Lin, H. Sun, X. Yang and Z. J. Guo, *Inorg. Chem.*, 2010, **49**, 2541.
62 F. J. M. Almes and D. Porschke, *Biochemistry*, 1993, **32**, 4246.
63 S. Tabassum, A. Asim, F. Arjmand, M. Afzal and V. Bagchi, *Eur. J. Med. Chem.*, 2012, **58**, 308.
64 M. Lee, A. L. Rhodes, M. D. Wyatt, S. Forrow and J. A. Hartley, *Biochemistry*, 1993, **32**, 4237.
65 K. Ghosh, P. Kumar, N. Tyagi, U. P. Singh, N. Goel, A. Chakraborty, P. Roy and M. C. Baratto, *Polyhedron*, 2011, **30**, 2667.
66 M. P. Fitzsimons and J. K. Barton, *J. Am. Chem. Soc.*, 1997, **119**, 3379.
67 S. Anbu, S. Kamalraj, B. Varghese, J. Muthumary and M. Kandaswamy, *Inorg. Chem.*, 2012, **51**, 5580.
68 C. Rajarajeswari, R. Loganathan, M. Palaniandavar, E. Suresh, A. Riyasdeen and M. A. Akbarshae, *Dalton Trans.*, 2013, **42**, 8347.
69 A. Kumar, J. P. Chinta, A. K. Ajay, M. K. Bhat and C. P. Rao, *Dalton Trans.*, 2011, **40**, 10865.
70 Y. J. Hu, Y. Liu, J. B. Wang, X. H. Xiao and S. S. Qu, *J. Pharm. Biomed. Anal.*, 2004, **36**, 915.
71 J. Lu, Q. Sun, J. L. Li, L. Jiang, W. Gu, X. Liu, J. L. Tian and S. P. Yan, *J. Inorg. Biochem.*, 2014, **137**, 46.
72 R. D. Senthil, N. S. P. Bhuvanesh and K. Natarajan, *Inorg. Chem.*, 2011, **50**, 12852.
73 J. Zhao, S. H. Gou, Y. Y. Sun, R. T. Yin and Z. M. Wang, *Chem. Eur. J.*, 2012, **18**, 14276.